DNA Research, 2018, 25(3), 307–315
doi: 10.1093/dnares/dsy003
Advance Access Publication Date: 30 January 2018
Full Paper

Full Paper

The genomes of two *Eutrema* species provide insight into plant adaptation to high altitudes

Xinyi Guo[1,†], Quanjun Hu[1,†], Guoqian Hao[1,2], Xiaojuan Wang[1], Dan Zhang[1], Tao Ma[1], and Jianquan Liu[1,*]

[1]Key Laboratory of Bio-Resource and Eco-Environment of Ministry of Education, College of Life Sciences, Sichuan University, Chengdu 610065, PR China, and [2]Management Committee for Emei Mountain Scenic Area, Biodiversity Institute of Emei Mountain, Leshan 614200, Sichuan, PR China

*To whom correspondence should be addressed. Tel. +028 8541 2053. Fax. +028 8541 2053. Email: liujq@nwipb.cas.cn
[†]Equal contributions to this work.

Edited by Dr Satoshi Tabata

Received 16 October 2017; Editorial decision 15 January 2018; Accepted 24 January 2018

Abstract

Eutrema is a genus in the Brassicaceae, which includes species of scientific and economic importance. Many *Eutrema* species are montane and/or alpine species that arose very recently, making them ideal candidates for comparative studies to understand both ecological speciation and high-altitude adaptation in plants. Here we provide *de novo* whole-genome assemblies for a pair of recently diverged perennials with contrasting altitude preferences, the high-altitude *E. heterophyllum* from the eastern Qinghai-Tibet Plateau and its lowland congener *E. yunnanense*. The two assembled genomes are 350 Mb and 412 Mb, respectively, with 29,606 and 28,881 predicted genes. Comparative analysis of the two species revealed contrasting demographic trajectories and evolution of gene families. Gene family expansions shared between *E. heterophyllum* and other alpine species were identified, including the disease resistance R genes (NBS-LRRs or NLRs). Genes that are duplicated specifically in the high-altitude *E. heterophyllum* are involved mainly in reproduction, DNA damage repair and cold tolerance. The two *Eutrema* genomes reported here constitute important genetic resources for diverse studies, including the evolution of the genus *Eutrema*, of the Brassicaceae as a whole and of alpine plants across the world.

Key words: *Eutrema*, high-altitude adaptation, *de novo* assembly, comparative genomics

1. Introduction

Adaptation to high altitude has contributed to the high level of plant and animal species biodiversity found on numerous mountains across the world.[1] It is well known that animals (including humans) living in highlands have evolved unique genetic adaptations in order to maintain oxygen homeostasis.[2] In plants, UV-B tolerance and cold tolerance appear to be critical for survival at high altitude.[3] However, the genetic mechanisms by which immobile plants adapt to high-altitude conditions remain largely unknown due to a lack of appropriate genome resources.

Species of the Brassicaceae family have a wide range of global distributions and adaptations, as well as different life histories and mating systems, and they therefore comprise an ideal system for many types of study.[4,5] Genome resources are critically important for all these studies.[6,7] Recent advances in high-throughput sequencing technology have facilitated the ability of the scientific community to sequence the genomes of an increasing number of Brassicaceae species for multiple purposes.[8–10] A previous genome study of an alpine polyploid Brassicaceae species suggested that expansion of numerous gene families was correlated with increased tolerance of cold and of UV-B stress.[3] However, such expansions may have arisen purely from genome duplications rather than because of high-altitude adaptations.

Eutrema is a genus in the Brassicaceae that contains more than 30 species, most of which are distributed in eastern Asia. In addition to the model plant *E. salsugineum* (Pall.) Al-Shehbaz & Warwick, which is used for studies of abiotic stress, and the commercial crop wasabi, *E. japonicum* (Miq.) Koidz, the genus contains numerous montane and/or alpine species.[11] Most of these species occur in the Qinghai-Tibet Plateau (QTP) and have originated recently in response to geologic and climatic changes since the Pliocene.[12] In this study, we report the *de novo* genome sequence assembly and comparative genomic analysis of an alpine plant, *E. heterophyllum*, from the eastern QTP, and its lowland congener, *E. yunnanense*, both of which originated from a very recent common ancestor and are diploid perennials with chromosome numbers of $2n = 14$ and similar selfing breeding systems,[12] therefore providing an ideal basis for genetic comparisons without the complicating effects of either genome duplication or phylogenetic evolution. In addition, these two genome assemblies provide important genetic resources for future comparative studies of this genus and family and of high-altitude adaptation in alpine plants.

2. Materials and methods

2.1. Plant materials, genomic DNA and total RNA extraction

We selected and sequenced a pair of *Eutrema* species that met three criteria: (1) diploid ($2n = 14$), (2) having diverged recently and (3) growing at contrasting altitudes in their natural distributions (Supplementary Fig. S1). One individual of *E. heterophyllum* was collected in June 2015 at the Zhuodala pass (∼4,700 m above sea level; asl) in Ganzi County, Sichuan Province, China. Fresh and healthy leaves, flowers and root were harvested and immediately frozen in liquid nitrogen, followed by storage at −80 °C in the laboratory prior to DNA/RNA extraction. For comparison, fresh samples of leaf, leafstalk and root tissues were obtained from one *E. yunnanense* plant collected in April 2014, from Xinning County (∼600 m asl), Hunan Province, China. We used the CTAB method to extract high-quality genomic DNA from 5 g of leaf tissues for each species. The quality of the high-molecular weight DNA was checked by 1% agarose gel electrophoresis. Around 200 μg of genomic DNA was used for library construction. We extracted total RNA with RNAiso Plus reagent (Takara, Japan) for each tissue collected from both species (i.e. leaves, flowers and roots for *E. heterophyllum*, and leaves, leafstalks and roots for *E. yunnanense*). The quality of the extracted RNA was verified by 1% agarose gel. DNase treatment was performed before library construction. For each sample, 5 μg of the total high-quality RNA was used for sequencing.

2.2. Genome sequencing and assembly

We constructed Illumina libraries with small (200-, 500- and 800-bp) and large (2-, 5-, 10- and 20-kb) inserts and then sequenced them following the Illumina protocols (Illumina, San Diego, CA) using the Illumina HiSeq X Ten platform at Novogene (Tianjin, China). Short reads were first subjected to quality filtering using Trimmomatic v0.33,[13] error correction using BFC (version r181)[14] and mate-pair data deduplication using FastUniq v1.1.[15] We then used SOAPec v2.01[16] to estimate the genome size as well as the level of genome-wide heterozygosity, which was based on the 17-mer frequency distribution. We adopted the Platanus[17] pipeline, which can efficiently assemble genomes with various levels of heterozygosity. Both genomes were initially assembled into scaffolds using Platanus (version 1.2.2)[17] with the first round of gap closing. An additional gap closing procedure was performed with GapCloser (version 1.12).[16] Finally we evaluated genome assemblies for gene coverage using the CEGMA[18] and BUSCO (version 2.0)[19] pipeline.

2.3. Repeat identification

To structurally annotate repeat sequences in the two *Eutrema* genomes, we used the TEdenovo pipeline from the REPET package (v2.5) with default parameters.[20] The pipeline performed a self-comparison for the input genome using the BLASTER software (version 2.25)[21] to identify and classify repeated elements. In order to attain more comprehensive prediction of TEs, we employed the pipeline to carry out structural detection analysis using LTRharvest (version 1.5.8).[22] RECON v1.0.8,[23] PILER v1.0[24] and GROUPER v2.27[21] were then employed to cluster the matches detected. By performing a multiple sequence alignment using the Map algorithm,[25] a consensus sequence for each cluster was generated to represent the ancestral TE. These consensus sequences were then classified by looking for characteristic structural features and similarities to known TEs in Repbase (20.05),[26] and by scanning against the Pfam library[27] with HMMER3.[28] To annotate all TEs across the genome, we further employed the TEannot pipeline[21] with the default parameters. This pipeline mines the genome sequence using repeated sequences identified in the previous TEdenovo pipeline to produce classified non-redundant consensus repeat sequences along with short simple repeats, which are exported in GFF3 format. We followed the method of Maumus and Quesneville[29] to calculate the age of repetitive DNAs.

2.4. Gene prediction

A combination of *ab initio*, homology-based and transcript-based methods was used for gene prediction. We first built a comprehensive transcriptome database with the PASA pipeline.[30] After quality control with Trimmomatic v0.33,[13] Illumina RNA-seq reads were assembled into *de novo* transcripts using Trinity.[31] Then two sets of genome-guided transcripts were built using (1) the genome-guided mode implemented in Trinity and (2) the HISAT-StringTie pipeline.[32] We performed *ab initio* prediction with Augustus (v3.2.2)[33] using *Arabidopsis thaliana* as the species model and our comprehensive transcriptome dataset as the input cDNA hint. We used GlimmerHMM (v3.0.4)[34] with the pre-trained directory for *A. thaliana* genes to generate another set of *ab initio* predictions. For homology-based prediction, protein sequences of 26,531 *E. salsugineum* genes[35] as well as the UniRef90 dataset[36] for all Brassicaceae species were aligned to the genome assemblies using SPALN2.[37] Gene models from the three main sources (i.e. aligned transcripts, *ab initio* predictions and aligned proteins) were merged to produce consensus models by EVidenceModeler.[30] Weights of evidences for gene models were manually set as: *ab initio* predictions, weight (Augustus) = 1 and weight (GlimmerHMM) = 1; protein alignments, weight (*E. salsugineum*) = 2 and weight (Brassicaceae_UniRef90) = 1; transcripts, weight (PASA) = 10. The EVM consensus predictions were updated by performing an additional round of PASA annotation in order to add UTR and alternatively spliced isoform annotations to gene models.

2.5. Functional annotation

We used BlastP[38] (with *E*-value $\leq 1 \times 10^{-5}$) to assign functional descriptions by carrying out sequence homology searches against different sources, including protein datasets from SwissProt[39] and the *Arabidopsis* genome annotation version TAIR10[40]. Motifs and domains within gene models were identified by deploying InterProScan (version 5.20.29)[41] with the options -dp -goterms -iprlookup -pathways -t p against multiple publicly available databases (Pfam, PROSITE, PRINTS, SMART, TIGRFAMs, Gene3D, PANTHER, etc.). We used AHRD (https://github.com/groupschoof/AHRD (24 January 2018, date last accessed)) to gather information from the search results and added Gene Ontology (GO) information using the GO annotation database[42] for *A. thaliana* (https://www.ebi.ac.uk/GOA/arabidopsis_release; (24 January 2018, date last accessed)).

2.6. Comparative genomic analysis

We downloaded the protein-coding genes of 13 Brassicaceae species (*A. thaliana*, *A. lyrata*, *Brassica rapa*, *Capsella rubella*, *Leavenworthia alabamica*, *Sisymbrium irio*, *Aethionema arabicum*, *Arabis alpina*, *Raphanus raphanistrum*, *Cardamine hirsuta*, *Schrenkiella parvula*, *Thlaspi arvense*, *E. salsugineum*; see Supplementary Table S4). We used OrthoMCL[43] to delineate gene families and cluster all genes into paralogous and orthologous groups. Gene family expansion and contraction analysis was performed with CAFE3 software.[44] Functional enrichment analysis was carried out by agriGO v2.0.[45] We used R[46] to perform clustering analysis for the gene families of the greatest size in *E. heterophyllum*. The transformed *z*-score profile was obtained from the number of genes per species for each family, and the hierarchically clustered (complete linkage clustering) ones, using Pearson correlation as a distance measure. The 2,235 single-copy gene families were used to reconstruct phylogenies with RAxML.[47] Alignment of protein sequences was performed with PRANK[48] and they were then back translated into coding sequences with PAL2NAL.[49] The MCMCtree program within the PAML package v4.9a[50] was used to estimate divergence time. The split of the two major lineages within the Brassicaceae was constrained to be between 20 and 30 million years ago.[51] We used MCScanX[52] to call intra- and inter-species gene collinearity. Synonymous substitutions were calculated for aligned gene pairs within identified collinearity blocks using the codeml program implemented in PAML.

2.7. SNP calling and demographic history reconstruction

We used the pairwise sequentially Markovian coalescent (PSMC) model[53] to estimate the history of effective population sizes (Ne) based on genome-wide diploid sequence data. This method has been previously applied to human and other vertebrates, as well as plants, for inferring demographic histories over long evolutionary periods. The quality-filtered Illumina pair end reads with insert sizes of ~500 bp for each species were mapped to the corresponding genome assemblies using BWA (version 0.7.10-r789).[54] For SNP calling, we used the SAMtools (v1.4) pipeline.[55] The settings for PSMC analysis (-p and -t options) were chosen manually according to suggestions given by the authors (https://github.com/lh3/psmc (24 January 2018, date last accessed)). We also performed 100 rounds of bootstrapping with the same parameters. The results were combined and plotted using the plot tool in PSMC. A generation time of 3 years and a mutation rate of 7×10^{-9} per site per year were applied.

2.8. NLR genes and integrated domains

NLR (nucleotide-binding site with leucine-rich repeat) genes in the *E. heterophyllum* and *E. yunnanense* genomes were directly extracted from the InterProScan results using the Pfam domain of the nucleotide-binding adaptor shared by APAF-1, R proteins and CED-4 (NB-ARC, PF00931) as query. We further applied the same strategy to identify NLRs in protein sequences from 13 cruciferous species with genomes available. After excluding typical Pfam domains contained in NLRs (i.e. PF01582 for Toll/interleukin-1 receptor [TIR], PF13855 for leucine-rich repeat [LRR] and PF05659 for Resistance to Powdery Mildew 8 [RPW8]), we obtained a list of additional domains that were likely to be fused with NLR proteins. We did not detect TIR2 (PF13676) in our annotated NLRs; this is a TIR domain newly identified among NLR proteins.[56] However, most previously characterized gene fusions were recaptured in this study, indicating that the approach we used for domain searching was conservative and generally reliable. A maximum likelihood tree of phloem protein 2 domains was constructed with RAxML under the PROTGAMMA model with BLOSUM62 matrix, specifying 500 bootstrap replicates. The gene tree was visualized in FigTree v1.4.2 (http://tree.bio.ed.ac.uk/software/figtree/ (24 January 2018, date last accessed)).

2.9. Positive selection in *SCC3* genes

The ratio of non-synonymous substitutions per non-synonymous site (dN) to synonymous substitutions per synonymous site (dS), or ω, is a commonly used indicator of selective pressure acting on protein-coding genes, with $\omega > 1$ representing positive selection, $\omega = 1$ representing neutral evolution and $\omega < 1$ representing purifying selection. To identify signals of positive selection, we extracted *SCC3* sequences from all Brassicaceae genomes. A gene tree of aligned protein sequences was constructed using RAxML under the PROTGAMMA model with BLOSUM62 matrix, specifying 500 bootstrap replicates. We used codeml in the PAML software package (v4.9a) to perform the branch-site test among duplicated *SCC3* paralogs for a series of pairs of alternative versus null models, aiming to find out whether or not any proportion of coding sites within each paralog has $\omega > 1$ compared with the background level. Log-likelihood values for each pair of nested models were compared using the likelihood ratio test (LRT) to obtain the *P*-value of significance.

3. Results

3.1. Genome assembly and annotation

After Illumina sequencing and quality control, we obtained 111.87 and 97.29 Gb of Illumina short reads from seven sequencing libraries, corresponding to an estimated 249× and 230× base-pair coverage, for *E. heterophyllum* and *E. yunnanense*, respectively (Supplementary Table S1). The estimated genome size of ~400 Mb for both species is larger than that of their congener *E. salsugineum*,[35] with a higher level of genome-wide heterozygosity in the low-altitude species *E. yunnanense* (Supplementary Fig. S2). A *de novo* assembly pipeline allowed us to generate genome assemblies that captured 350 and 413 Mb in 149,415 and 317,771 contigs for the two *Eutrema* genomes, of which 328 and 386 Mb (81% and 91% of the estimated genome sizes) were represented in scaffolds of

1 kb or greater (Table 1). Repetitive DNA constitutes 67% and 70% of, respectively, the *E. heterophyllum* and the *E. yunnanense* genome. Long terminal repeat (LTR) retrotransposons are the most abundant among these repetitive sequences (Supplementary Table S2), having contributed to a recent wave of TE burst (Kimura divergence ≤ 5, Supplementary Fig. S3). Gene completeness analysis revealed that we had achieved more than 95% completeness of gene coverage for both genomes (Supplementary Table S3). We predicted 29,606 genes for *E. heterophyllum* and 28,881 for *E. yunnanense* (Table 1). Clustering of predicted proteomes for 15 Brassicaceae genomes yielded a total of 27,193 gene families, which comprised 380,484 genes (~85% of all 448,886 genes; see Supplementary Table S4).

Table 1. Genome assembly and annotation statistics for two *Eutrema* species

	E. heterophyllum	*E. yunnanense*
Assembly statistics		
Estimated genome size (Mb)	405	423
Number of contigs	149,415	317,771
Contig length (Mb)	350.47	412.62
Longest contig (Mb)	0.67	0.39
Contig L50 (seqs)	1264	3269
Contig N50 (kb)	74.65	32.56
Number of scaffolds (>1 kb)	7,690	14,031
Scaffold length (Mb)	328.16	385.58
Longest scaffold (Mb)	3.5	2.07
Scaffold L50 (seqs)	189	341
Scaffold N50 (kb)	535.32	331.5
Annotation statistics		
Number of gene models	29,606	28,881
With InterPro annotations	22,593	22 343
With GO annotations	20,879	20,254
Mean CDS size (bp)	1201.3	1222.3
Mean exon size (bp)	291.5	301.3
Mean intron size (bp)	233.0	210.6

3.2. Comparative phylogenomics and demographic histories

We analysed the phylogenetic relationships of 15 Brassicaceae species (Supplementary Table S4) using four-fold degenerate third-codon transversion (4DTv) sites in 2,193 one-to-one orthologous genes identified across their genomes. The nuclear-genome phylogeny (Fig. 1; Supplementary Fig. S4) is congruent with the plastome phylogeny reported previously.[51] We dated the divergence of the two species to 3.5 (1.5–7.2) Mya (Fig. 1; Supplementary Fig. S5). Clustering analysis of gene family size revealed that many duplicated genes were retained in genomes known to be polyploid (Fig. 1). We failed to detect any additional whole genome duplication in the two *Eutrema* species when compared with *A. thaliana* using synonymous substitutions per synonymous site (dS) age distribution analysis (Supplementary Fig. S6). We identified 581,883 and 807,391 heterozygous sites in, respectively, the *E. heterophyllum* and the *E. yunnanense* genome. Consistent with the results of analysing K-mer frequency distribution (Supplementary Fig. S2), *E. heterophyllum* had a lower heterozygous SNP rate (1.75 × 10^{-3}) than *E. yunnanense* (2.18 × 10^{-3}). A sharp peak was observed in the distribution of genome-wide SNP density for *E. heterophyllum* (Fig. 2A), suggesting that mutations within this genome are more evenly distributed than those in the *E. yunnanense* genome. PSMC analysis based on the local SNP densities of heterozygous sites revealed distinct demographic histories for the two species, in that the high-altitude *E. heterophyllum* showed a decrease-increase-decrease trend while the population size of the low-altitude *E. yunnanense* decreased continuously in the recent past (Fig. 2B).

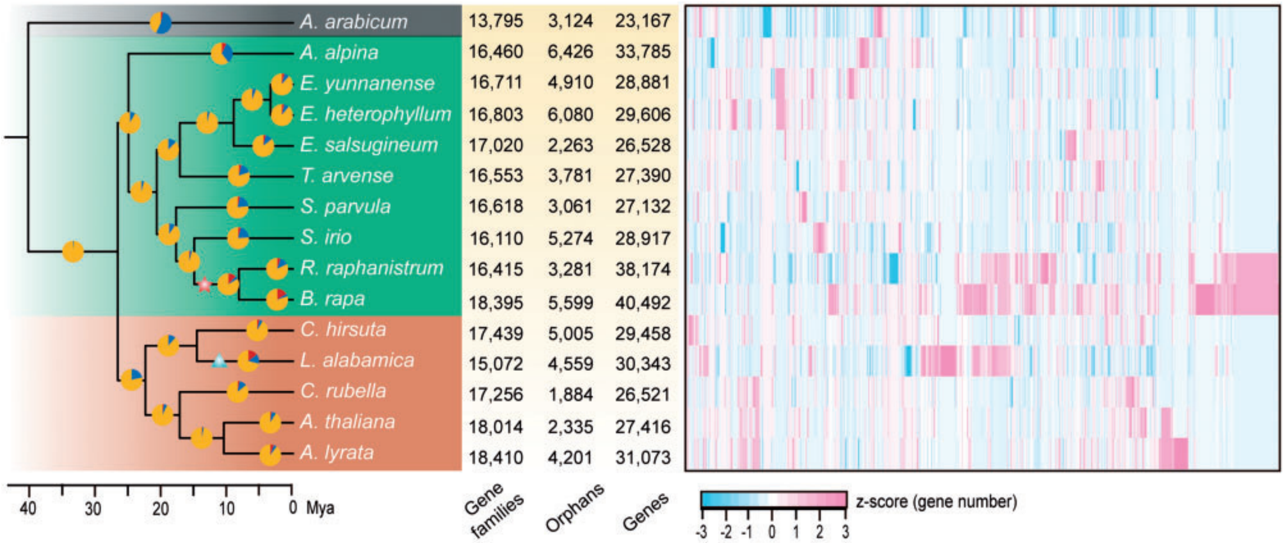

	Gene families	Orphans	Genes
A. arabicum	13,795	3,124	23,167
A. alpina	16,460	6,426	33,785
E. yunnanense	16,711	4,910	28,881
E. heterophyllum	16,803	6,080	29,606
E. salsugineum	17,020	2,263	26,528
T. arvense	16,553	3,781	27,390
S. parvula	16,618	3,061	27,132
S. irio	16,110	5,274	28,917
R. raphanistrum	16,415	3,281	38,174
B. rapa	18,395	5,599	40,492
C. hirsuta	17,439	5,005	29,458
L. alabamica	15,072	4,559	30,343
C. rubella	17,256	1,884	26,521
A. thaliana	18,014	2,335	27,416
A. lyrata	18,410	4,201	31,073

Figure 1. Dated phylogeny and gene family analysis of Brassicaceae species. Pie charts showing gains (red) and losses (blue) of gene families are indicated along branches and nodes. The numbers of gene families, orphans (single-copy gene families) and predicted genes, as well as a heat map depicting the hierarchically clustered *z*-score profile for gene numbers within each family, is indicated next to each species. Background colours on the phylogenetic tree (top to bottom) are basal clade, lineage II and lineage I Brassicaceae species, respectively. Full species names: *Aethionema arabicum*, *Arabis alpina*, *Eutrema yunnanense*, *Eutrema heterophyllum*, *Eutrema salsugineum*, *Thlaspi arvense*, *Schrenkiella parvula*, *Sisymbrium irio*, *Raphanus raphanistrum*, *Brassica rapa*, *Cardamine hirsuta*, *Leavenworthia alabamica*, *Capsella rubella*, *Arabidopsis thaliana*, *Arabidopsis lyrata*. The star and triangle denote lineage-specific whole-genome triplications. Mya, million years ago. See online version for color display.

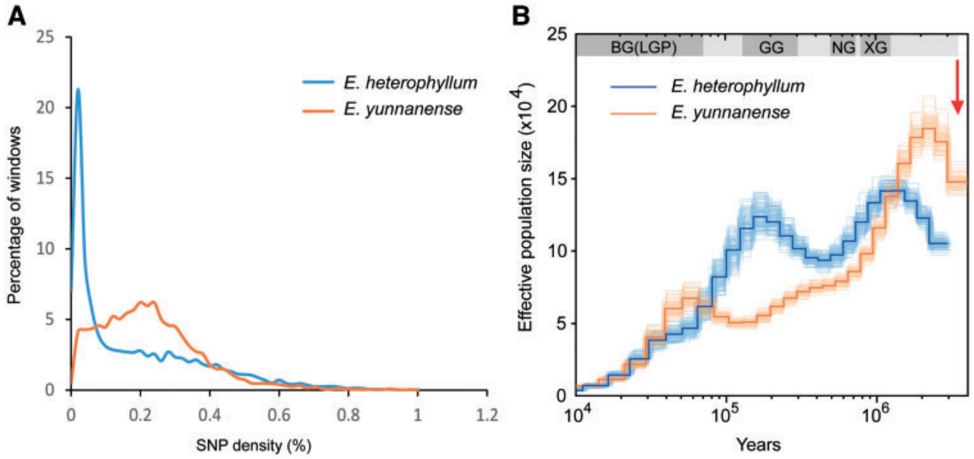

Figure 2. SNP density distribution and demographic history of two *Eutrema* species. (A) Distribution of SNP density across each *Eutrema* genome. Heterozygous SNPs were counted and used to calculate heterozygosity density in non-overlapping 50-kb windows. (B) PSMC inference of ancestral effective population size change in the two species. The estimated ancestral population sizes are represented by central bold lines, and the PSMC estimations of 100 bootstraps resampled from the original sequence are represented by thin curves surrounding each line. A generation time of 3 years and a mutation rate of 7×10^{-9} per site per year were assumed for both species. Dark grey and abbreviations indicate glaciation periods, while light grey corresponds to interglaciation. BG (LGP), Baiyu Glaciation (last glaciation period, 70 ~ 10 thousand years ago, kya); GG, Guxiang Glaciation (300 ~ 130 kya); NG, Naynayxungla Glaciation (780 ~ 500 kya); XG, Xixiabangma Glaciation (1,170 ~ 800 kya). Red arrow denotes the estimated divergence time of the two species.

3.3. Expansion of NLR genes and analysis of domain integration

In comparison with other Brassicaceae species, we found that 141 and 178 gene families had significantly expanded ($P < 0.05$) in the *E. heterophyllum* and *E. yunnanense* genomes, respectively (Supplementary Tables S5–S8). Among the gene families that had expanded within the high-altitude *E. heterophyllum*, GO terms including 'response to stress' and 'nucleotide binding' (adjusted $P < 0.05$, Supplementary Fig. S7) were overrepresented, while no particular GO term was enriched in the case of the low-altitude *E. yunnanense*. The terms enriched in *E. heterophyllum* could be largely attributed to 10 clusters of disease resistance genes encoding nucleotide-binding site with leucine-rich repeat (NLR) proteins (Supplementary Table S6). We noticed that most of these NLR gene families had also expanded in the genomes of three other Brassicaceae species, *A. alpina*, *A. lyrata* and *C. hirsuta*, of which the former two are well documented as alpine plants (Fig. 3). Two NLR families shared across these species account for ~20% of the total number of NLR genes that differ between *E. heterophyllum* and *E. yunnanense* (Supplementary Table S5). Overall, the gene families expanded in *E. heterophyllum* overlap significantly with those expanded in each of these three species ($P < 0.01$, Fisher's exact test) (Fig. 3; Supplementary Fig. S8). These results imply that parallel expansion of gene sets, particularly within the NLR genes, may have repeatedly occurred in alpine plants.

Plant NLR genes can fuse with additional domains (hereafter referred to as NB-IDs) that serve as 'baits' for pathogen-derived molecules.[56] We identified 112 NB-IDs with 82 distinct integrated domains across the Brassicaceae genomes (Supplementary Fig. S9; Supplementary Table S9). Within the fused domains, 22 were present in at least two genomes (Supplementary Table S10). Interestingly, in *E. heterophyllum*, we found that integration of one domain encoding phloem protein 2 (PP2, Pfam ID: PF14299), characteristic of a group of plant lectins involved in responses to various stresses,[57] was shared by two other species, *A. alpina* and *C. hirsuta* (Fig. 4). It is worth noting that the NLRs fused with this domain were clustered into the same gene family that had undergone expansion in all these genomes (Supplementary Table S5). Obviously, the fusion of PP2 arose independently in these three species (Fig. 4), probably in response to the same class of pathogens.

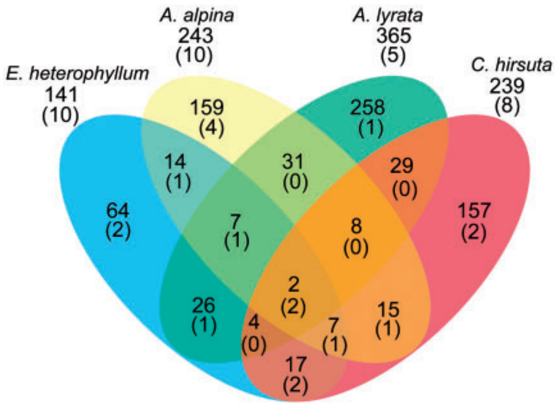

Figure 3. Shared gene family expansions among four Brassicaceae species. Venn diagram showing overlap of shared gene families and of the nuclear-binding site with leucine-rich repeats (NLR) genes. Numbers of significantly expanded gene families among the four genomes that contain the largest number of NLRs are shown. Counts of the significantly expanded NLR gene families are given in parentheses.

3.4. Species-specific gene duplications and high-altitude adaptation

We also analysed the functional enrichment of genes that were duplicated specifically in the high- or low-altitude species. In the high-altitude *E. heterophyllum*, we observed 30 enriched GO terms within the biological process ontology, including 'response to stimulus', 'response to stress', 'reproductive process' and 'cell cycle'. However, only four terms within the biological process ontology, 'developmental process', 'anatomical structure development', 'multicellular organism development' and 'multicellular organismal process', were

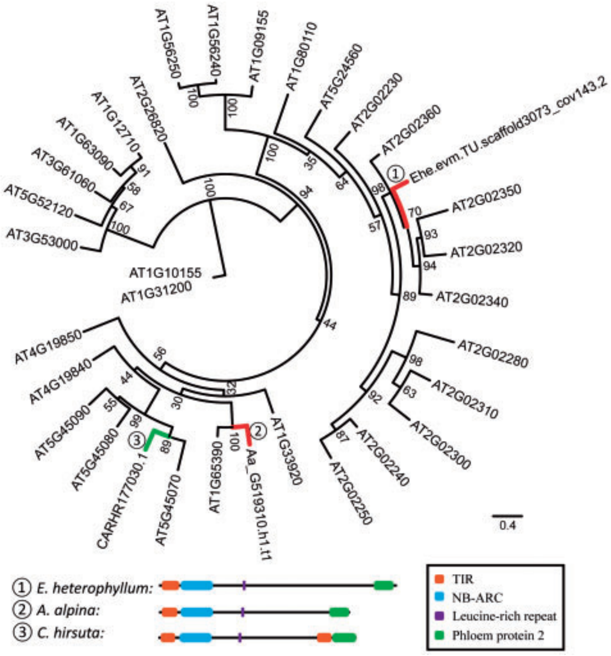

Figure 4. Phylogeny of the phloem protein 2 (PP2) domain fused with expanded NLR genes. Sequences from all *A. thaliana* proteins containing this domain and the integrated PP2 detected in three Brassicaceae genomes (labelled with numbers within circles) were analyzed. Branches are coloured red if a species has a documented high-altitude distribution, and green if not. The structure of NLR fused with PP2 is shown below the gene tree. See online version for color display.

recovered for the low-altitude *E. yunnanense* (Supplementary Tables S11–S14).

A close examination of the families expanded in *E. heterophyllum* revealed multiple genes that are involved in plant reproduction and DNA damage repair (DDR), probably in response to UV-B radiation and other abiotic stresses imposed by the harsh alpine environment. For example, more copies were found for *NBS1*, *RPA32* and *SNI1*, which are involved in homologous recombination (HR) using the intact sister chromatid, and *KU80* and *XRCC4*, which participate in the non-homologous end-joining (NHEJ) process (Fig. 5A, Supplementary Table S11); HR and NHEJ are the two major pathways for the repair of double-strand breaks.[58] Duplicated genes involved in the regulation of the cell cycle (*SIM*, *ATXR5* and *ICK3*) were also detected for *E. heterophyllum* (Fig. 5A, Supplementary Table S11); SIM is a plant-specific CDK inhibitor binding CDKB1; 1, probably specifically controlling endocycle onset during the G2/M transition.[59]

Of the genes with the largest family sizes (*z*-score normalized) in *E. heterophyllum*, two (*SCC3* and *SMC3*) encode subunits of the cohesin complex, a well-known ring-shaped molecule with a critical role in sister chromatid cohesion.[60] In *E. heterophyllum*, we found four copies of *SCC3* and three ones of *SMC3* (Fig. 5B). Most of these copies were expressed in leaf, root and/or flower tissue (Fig. 5B). A duplication of *SCC3* was also found in *A. lyrata*, another alpine crucifer species (Fig. 6). Using the branch-site model, we showed that duplicated *SCC3* copies were under positive selection (Fig. 6). The average pairwise identity between the amino acid sequences of the *SCC3* genes in the high-altitude *E. heterophyllum* is only 61.1%, indicating that the duplication of this gene may have occurred very early. Intriguingly, although only one intact *SCC3* gene was found in the low-altitude *E. yunnanense*, multiple *SCC3* fragments were identified (Supplementary Fig. S10). Of these, one fragment was found within gene pairs that are collinear between the two *Eutrema* species (Supplementary Fig. S11). These findings suggest that duplication of *SCC3* arose before the divergence of these species and subsequent pseudogenization may have occurred in *E. yunnanense*.

Three genes, *ICE2*, *FAB1* and *VIN3*, involved in cold stress was also observed to be duplicated in the high-altitude *E. heterophyllum* (Supplementary Table S11). *ICE2* encodes a transcription factor that confers rapid freezing tolerance in *A. thaliana*.[61] The product of *FAB1* is involved in membrane lipid synthesis and photosynthesis collapses in the *Arabidopsis fab1* mutant due to degradation of chloroplasts when plants are exposed to low temperature for long periods.[62,63] *VIN3*, which is induced by prolonged winter cold, is essential for the repression of *FLC* during vernalization.[64]

4. Discussion

In this study, we performed *de novo* genome assemblies for *E. heterophyllum* and *E. yunnanense*, a pair of diploid perennials, which have diverged recently but have contrasting altitude preferences. Compared with previously published Brassicaceae genomes that were assembled from Illumina short reads,[8,65] our genome assemblies were of high quality in terms of continuity and gene coverage, making them suitable for subsequent comparative genomic analysis and thus representing important genetic resources. Phylogenomic analysis confirmed the close relationship and the diploid nature of these two *Eutrema* species. However, the contrasting demographic histories of the two species may reflect their different responses to the local climatic oscillations that occurred during the Quaternary. The dramatic genomic differences observed here may have partly contributed to the high- or low-altitude adaptations that they exhibit.

The NLRs are among the most variable genes across plant species. Variation in these genes between high- and low-altitude *A. thaliana* populations was discovered recently.[66] We found an increase in the number of gene copies for some NLR groups in *E. heterophyllum* and other alpine species of the family Brassicaceae. In addition, we identified a fused domain encoding PP2 among these expanded NLR genes and confirmed the independent acquisition of this domain in different species. According to a recent comprehensive study of fused domains in plant species, this domain also exists in NLRs of Malvaceae and Poaceae species.[56] Thus members of the PP2 family have fused with NLR genes multiple times in different angiosperm lineages. Further studies are needed to investigate whether and how plant immune receptors are involved in high-altitude adaptation in other alpine species.

In the high-altitude *E. heterophyllum*, we found that many genes related to reproduction and DDR had undergone duplications, probably in response to abiotic stress. It should be noted that most of these reproduction-related genes remain as single copies in most angiosperms.[67] In addition, two genes in this category (*SCC3* and *SMC3*) that have undergone duplication events encode cohesin subunits, and similar copy number variations have also been found in animals, where they may cause distinct functional changes in the cohesin complex.[68–71] To the best of our knowledge, this is the first report of duplication and possible subfunctionalization of cohesin subunits in plants. We have further shown that duplications of *SCC3* in *Eutrema* species occurred early, before their divergence. Although we cannot exclude the possibility that the apparent multiple partial *SCC3* sequences identified in *E. yunnanense* may be due to the fragmented nature of the draft genome, the evidence for

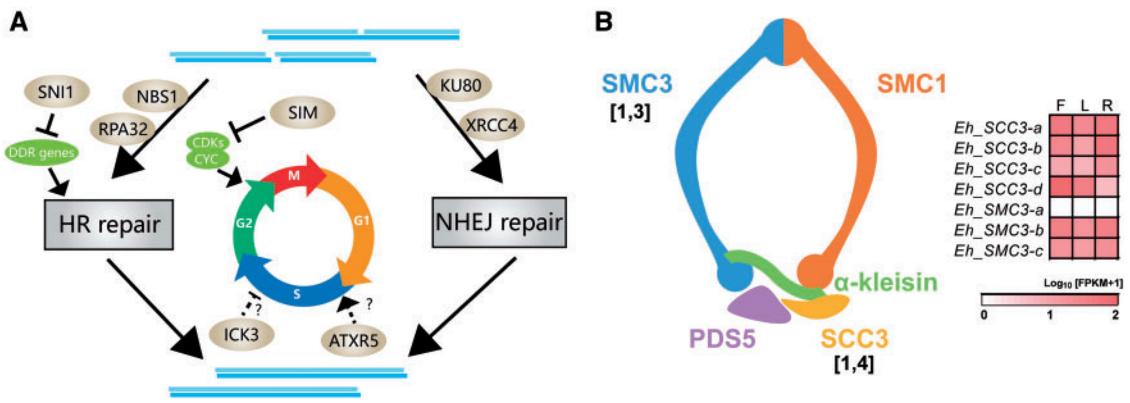

Figure 5. Duplication of genes related to DDR in *E. heterophyllum*. (A) Genes involved in the DDR pathway and cell cycle control that are duplicated in *E. heterophyllum*. Duplicated genes are shown in light brown. HR, homologous recombination; NHEJ, non-homologous end-joining. (B) A schematic picture of the plant cohesin complex indicating duplication of genes encoding two cohesin subunits, *SCC3* and *SMC3*. The numbers of the corresponding genes in *E. yunnanense* and *E. heterophyllum* are shown in square brackets in the format [*E. yunnanense*, *E. heterophyllum*]. The expression profiles in FPKM (fragments per kilobase per million reads mapped) of paralogs are plotted as $\log_{10}$ values. See online version for color display.

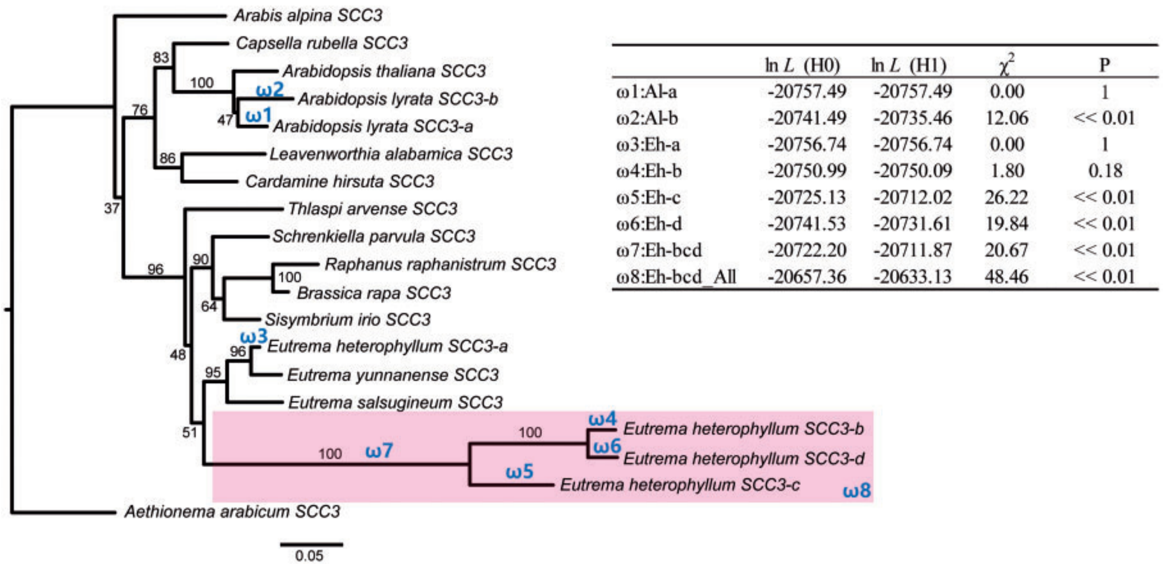
Arabis alpina SCC3
Capsella rubella SCC3
Arabidopsis thaliana SCC3
Arabidopsis lyrata SCC3-b
Arabidopsis lyrata SCC3-a
Leavenworthia alabamica SCC3
Cardamine hirsuta SCC3
Thlaspi arvense SCC3
Schrenkiella parvula SCC3
Raphanus raphanistrum SCC3
Brassica rapa SCC3
Sisymbrium irio SCC3
Eutrema heterophyllum SCC3-a
Eutrema yunnanense SCC3
Eutrema salsugineum SCC3
Eutrema heterophyllum SCC3-b
Eutrema heterophyllum SCC3-d
Eutrema heterophyllum SCC3-c
Aethionema arabicum SCC3
83
100
76
47
86
37
96
90
100
64
48
96
95
51
100
100
ω1
ω2
ω3
ω4
ω5
ω6
ω7
ω8
0.05

	ln *L* (H0)	ln *L* (H1)	χ^2	P
ω1:Al-a	-20757.49	-20757.49	0.00	1
ω2:Al-b	-20741.49	-20735.46	12.06	<< 0.01
ω3:Eh-a	-20756.74	-20756.74	0.00	1
ω4:Eh-b	-20750.99	-20750.09	1.80	0.18
ω5:Eh-c	-20725.13	-20712.02	26.22	<< 0.01
ω6:Eh-d	-20741.53	-20731.61	19.84	<< 0.01
ω7:Eh-bcd	-20722.20	-20711.87	20.67	<< 0.01
ω8:Eh-bcd_All	-20657.36	-20633.13	48.46	<< 0.01

Figure 6. Phylogenetic relationships and positive selection of *SCC3* genes in Brassicaceae species. Values above branches indicates the support values obtained from 500 bootstrap replicates. Scale bar represents the number of substitutions per site. The branches tested in branch-sites tests of selection for the *EhSCC3* and *AlSCC3* genes are indicated. The inset table shows the results of the branch-sites tests, with a *P*-value based on 1 degrees of freedom. ln *L*, log-likelihood values; H0, null model; H1, alternative model; χ^2, chi-square test likelihood ratio (2Δln *L*).

pseudogenization in this species is strong. The duplication, followed by subsequent loss, of *SCC3* in *E. yunnanense* may be correlated with its initial occurrence (or its ancestral distribution) in the high-altitude QTP and subsequent migration to the lower-altitude region.[12] As the cohesin complex has a profound impact on reproduction as well as on gene regulation, duplication of these subunits may have played an important role in plant adaptation to harsh alpine environments. In addition, duplication of genes related to cold acclimation in the high-altitude *E. heterophyllum* may be correlated with plant adaptation to the low and rapidly changing temperatures experienced in alpine habitats.

In summary, we assembled *de novo* genomes of two *Eutrema* species and inferred genetic changes in the alpine species that may underlie high-altitude adaptation, although further tests in more species using multiple approaches are needed. The genome resources that we have developed for the two *Eutrema* species will be very useful for many studies in this genus, the Brassicaceae as a whole, and alpine plants in general.

Availability

The short reads of Illumina DNAseq and RNAseq generated in this study are available from the National Center for Biotechnology Information (NCBI) Short Read Archive (SRA) under BioProject PRJNA419026 (BioSample SAMN08200758 for *E. heterophyllum* and SAMN08200758 for *E. yunnanense*). The genome assemblies of this project have been deposited at DDBJ/ENA/GenBank under the accession PKMM00000000 for *E. heterophyllum* and PKML00 000000 for *E. yunnanense*.

Acknowledgements

We thank Bingbing Liu for his help in DNA extraction.

Funding

This work was supported by grants from the National Key Research and Development program (2017YFC0505203), National Natural Science Foundation of China (31590821), National Key Project for Basic Research (2014CB954100), Youth Science and Technology Innovation Team of Sichuan Province (2014TD003), and the 985 and 211 Projects of Sichuan University.

Conflict of interest

The authors declare that they have no competing interests.

Authors' contributions

J.L. conceived the study. G.H. and X.G. collected samples. X.G. and Q.H. assembled the genomes and performed genome annotation and evolutionary analyses with the help of X.W, D.Z. and T.M. X.G. and J.L. wrote the manuscript. All authors read and approved the final manuscript.

Supplementary data

Supplementary data are available at *DNARES* online.

References

1. Hughes, C. E. and Atchison, G. W. 2015, The ubiquity of alpine plant radiations: from the Andes to the Hengduan Mountains, *New Phytol.*, **207**, 275–82.
2. Beall, C. M. 2014, Adaptation to high altitude: phenotypes and genotypes, *Annu. Rev. Anthropol.*, **43**, 251–72.
3. Zhang, J., Tian, Y., Yan, L., et al. 2016, Genome of plant maca (*Lepidium meyenii*) illuminates genomic basis for high-altitude adaptation in the central Andes, *Mol. Plant.*, **9**, 1066–77.
4. Bailey, C. D., Koch, M. A., Mayer, M., et al. 2006, Toward a global phylogeny of the Brassicaceae, *Mol. Biol. Evol.*, **23**, 2142–60.
5. Koch, M. A., Dobeš, C., Kiefer, C., Schmickl, R., Klimeš, L. and Lysak, M. A. 2006, Supernetwork identifies multiple events of plastid trn F (GAA) pseudogene evolution in the Brassicaceae, *Mol. Biol. Evol.*, **24**, 63–73.
6. Koenig, D. and Weigel, D. 2015, Beyond the thale: comparative genomics and genetics of Arabidopsis relatives, *Nat. Rev. Genet.*, **16**, 285.
7. Nikolov, L. A. and Tsiantis, M. 2017, Using mustard genomes to explore the genetic basis of evolutionary change, *Curr. Opin. Plant Biol.*, **36**, 119–28.
8. Gan, X., Hay, A., Kwantes, M., et al. 2016, The *Cardamine hirsuta* genome offers insight into the evolution of morphological diversity, *Nat. Plants*, **2**, 16167.
9. Jiao, W. B., Accinelli, G. G., Hartwig, B., et al. 2017, Improving and correcting the contiguity of long-read genome assemblies of three plant species using optical mapping and chromosome conformation capture data, *Genome Res.*, **27**, 778–86.
10. Willing, E. M., Rawat, V., Mandáková, T., et al. 2015, Genome expansion of *Arabis alpina* linked with retrotransposition and reduced symmetric DNA methylation, *Nat. Plants*, **1**, nplants201423.
11. Al-Shehbaz, I. A. and Warwick, S. I. 2005, A synopsis of *Eutrema* (Brassicaceae), *Harvard Pap. Bot.*, **10**, 129–35.
12. Hao, G. Q., Al-Shehba, I. A., Ahani, H., et al. 2017, An integrative study of evolutionary diversification of *Eutrema* (Eutremeae, Brassicaceae), *Bot. J. Linn. Soc.*, **184**, 204–23.
13. Bolger, A. M., Lohse, M. and Usadel, B. 2014, Trimmomatic: a flexible trimmer for Illumina sequence data, *Bioinformatics*, **30**, 2114–20.
14. Li, H. 2015, BFC: correcting Illumina sequencing errors, *Bioinformatics*, **31**, 2885–7.
15. Xu, H., Luo, X., Qian, J., et al. 2012, FastUniq: a fast de novo duplicates removal tool for paired short reads, *PLoS One*, **7**, e52249.
16. Luo, R., Liu, B., Xie, Y., et al. 2012, SOAPdenovo2: an empirically improved memory-efficient short-read de novo assembler, *Gigascience*, **1**, 18.
17. Kajitani, R., Toshimoto, K., Noguchi, H., et al. 2014, Efficient de novo assembly of highly heterozygous genomes from whole-genome shotgun short reads, *Genome Res.*, **24**, 1384–95.
18. Parra, G., Bradnam, K. and Korf, I. 2007, CEGMA: a pipeline to accurately annotate core genes in eukaryotic genomes, *Bioinformatics*, **23**, 1061–7.
19. Simao, F. A., Waterhouse, R. M., Ioannidis, P., Kriventseva, E. V. and Zdobnov, E. M. 2015, BUSCO: assessing genome assembly and annotation completeness with single-copy orthologs, *Bioinformatics*, **31**, 3210–2.
20. Flutre, T., Duprat, E., Feuillet, C. and Quesneville, H. 2011, Considering transposable element diversification in de novo annotation approaches, *PLoS One*, **6**, e16526.
21. Quesneville, H., Bergman, C. M., Andrieu, O., et al. 2005, Combined evidence annotation of transposable elements in genome sequences, *PLoS Comput. Biol.*, **1**, 166–75.
22. Ellinghaus, D., Kurtz, S. and Willhoeft, U. 2008, LTRharvest, a efficient and flexible software for *de novo* detection of LTR retrotransposons, *BMC Bioinformatics*, **9**, 18.
23. Bao, Z. and Eddy, S. R. 2002, Automated *de novo* identification of repeat sequence families in sequenced genomes, *Genome Res.*, **12**, 1269–76.
24. Edgar, R. C. and Myers, E. W. 2005, PILER: identification and classification of genomic repeats, *Bioinformatics*, **21(suppl_1)**, i152–8.
25. Huang, X. 1994, On global sequence alignment, *Comput. Appl. Biosci.*, **10**, 227–35.
26. Bao, W., Kojima, K. K. and Kohany, O. 2015, Repbase Update, a database of repetitive elements in eukaryotic genomes, *Mob. DNA*, **6**, 11.
27. Finn, R. D., Coggill, P., Eberhardt, R. Y., et al. 2016, The Pfam protein families database: towards a more sustainable future, *Nucleic Acids Res.*, **44**, D279–85.
28. Eddy, S. R. 2008, A probabilistic model of local sequence alignment that simplifies statistical significance estimation, *PLoS Comp. Biol.*, **4**, e1000069.
29. Maumus, F. and Quesneville, H. 2014, Ancestral repeats have shaped epigenome and genome composition for millions of years in *Arabidopsis thaliana*, *Nat. Commun.*, **5**, 4104.
30. Haas, B. J., Salzberg, S. L., Zhu, W., et al. 2008, Automated eukaryotic gene structure annotation using EVidenceModeler and the Program to Assemble Spliced Alignments, *Genome Biol.*, **9**, R7.
31. Grabherr, M. G., Haas, B. J., Yassour, M., et al. 2011, Full-length transcriptome assembly from RNA-Seq data without a reference genome, *Nat. Biotechnol.*, **29**, 644–52.
32. Pertea, M., Pertea, G. M., Antonescu, C. M., Chang, T. C., Mendell, J. T. and Salzberg, S. L. 2015, StringTie enables improved reconstruction of a transcriptome from RNA-seq reads, *Nat. Biotechnol.*, **33**, 290–5.
33. Stanke, M., Diekhans, M., Baertsch, R. and Haussler, D. 2008, Using native and syntenically mapped cDNA alignments to improve *de novo* gene finding, *Bioinformatics*, **24**, 637–44.
34. Majoros, W. H., Pertea, M. and Salzberg, S. L. 2004, TigrScan and GlimmerHMM: two open source ab initio eukaryotic gene-finders, *Bioinformatics*, **20**, 2878–9.
35. Yang, R., Jarvis, D. E., Chen, H., et al. 2013, The reference genome of the halophytic plant *Eutrema salsugineum*, *Front. Plant Sci.*, **4**, 1–14.
36. Suzek, B. E., Wang, Y., Huang, H., McGarvey, P. B., Wu, C. H. and UniProt, C. 2015, UniRef clusters: a comprehensive and scalable alternative for improving sequence similarity searches, *Bioinformatics*, **31**, 926–32.
37. Iwata, H. and Gotoh, O. 2012, Benchmarking spliced alignment programs including Spaln2, an extended version of Spaln that incorporates additional species-specific features, *Nucleic Acids Res.*, **40**, e161.

38. Camacho, C., Coulouris, G., Avagyan, V., et al. 2009, BLAST+: architecture and applications, *BMC Bioinformatics*, **10**, 421.
39. UniProt, C. 2015, UniProt: a hub for protein information, *Nucleic Acids Res*., **43**, D204–12.
40. Lamesch, P., Berardini, T. Z., Li, D., et al. 2012, The Arabidopsis Information Resource (TAIR): improved gene annotation and new tools, *Nucleic Acids Res*., **40**, D1202–10.
41. Jones, P., Binns, D., Chang, H. Y., et al. 2014, InterProScan 5: genome-scale protein function classification, *Bioinformatics*, **30**, 1236–40.
42. Huntley, R. P., Sawford, T., Mutowo-Meullenet, P., et al. 2015, The GOA database: gene Ontology annotation updates for 2015, *Nucleic Acids Res*., **43**, D1057–63.
43. Li, L., Stoeckert, C. J. and Roos, D. S. 2003, OrthoMCL: identification of ortholog groups for eukaryotic genomes, *Genome Res*., **13**, 2178–89.
44. Han, M. V., Thomas, G. W., Lugo-Martinez, J. and Hahn, M. W. 2013, Estimating gene gain and loss rates in the presence of error in genome assembly and annotation using CAFE 3, *Mol. Biol. Evol*., **30**, 1987–97.
45. Tian, T., Liu, Y., Yan, H., et al. 2017, AgriGO v2.0: a GO analysis toolkit for the agricultural community, 2017 update, *Nucleic Acids Res*., **43**, W122–9.
46. R Core Team. 2016, R: a language and environment for statistical computing. In: *R Foundation for Statistical Computing*. Vienna, Austria. https://www.R-project.org/.
47. Stamatakis, A. 2014, RAxML version 8: a tool for phylogenetic analysis and post-analysis of large phylogenies, *Bioinformatics*, **30**, 1312–3.
48. Loytynoja, A. and Goldman, N. 2008, Phylogeny-aware gap placement prevents errors in sequence alignment and evolutionary analysis, *Science*, **320**, 1632–5.
49. Suyama, M., Torrents, D. and Bork, P. 2006, PAL2NAL: robust conversion of protein sequence alignments into the corresponding codon alignments, *Nucleic Acids Res*., **34**, W609–12.
50. Yang, Z. 2007, PAML 4: phylogenetic analysis by maximum likelihood, *Mol. Biol. Evol*., **24**, 1586–91.
51. Guo, X. Y., Liu, J. Q., Hao, G. Q., et al. 2017, Plastome phylogeny and early diversification of Brassicaceae, *BMC Genomics*, **176**, 1–9.
52. Wang, Y., Tang, H., DeBarry, J. D., et al. 2012, MCScanX: a toolkit for detection and evolutionary analysis of gene synteny and collinearity, *Nucleic Acids Res*., **40**, e49.
53. Li, H. and Durbin, R. 2011, Inference of human population history from individual whole-genome sequences, *Nature*, **475**, 493–6.
54. Li, H. and Durbin, R. 2009, Fast and accurate short read alignment with Burrows-Wheeler transform, *Bioinformatics*, **25**, 1754–60.
55. Li, H. 2011, A statistical framework for SNP calling, mutation discovery, association mapping and population genetical parameter estimation from sequencing data, *Bioinformatics*, **27**, 2987–93.
56. Sarris, P. F., Cevik, V., Dagdas, G., Jones, J. D. and Krasileva, K. V. 2016, Comparative analysis of plant immune receptor architectures uncovers host proteins likely targeted by pathogens, *BMC Biol*., **14**, 8.
57. Dinant, S., Clark, A. M., Zhu, Y., et al. 2003, Diversity of the superfamily of phloem lectins (phloem protein 2) in angiosperms, *Plant Physiol*., **131**, 114–28.
58. Hu, Z., Cools, T. and De Veylder, L. 2016, Mechanisms used by plants to cope with DNA damage, *Annu. Rev. Plant Biol*., **67**, 439–62.
59. Adachi, S., Minamisawa, K., Okushima, Y., et al. 2011, Programmed induction of endoreduplication by DNA double-strand breaks in Arabidopsis, *Proc. Natl. Acad. Sci. USA*., **108**, 10004–9.
60. Schubert, V. 2009, SMC proteins and their multiple functions in higher plants, *Cytogenet. Genome Res*., **124**, 202–14.
61. Fursova, O. V., Pogorelko, G. V. and Tarasov, V. A. 2009, Identification of *ICE2*, a gene involved in cold acclimation which determines freezing tolerance in *Arabidopsis thaliana*, *Gene*, **429**, 98–103.
62. Wu, J., Lightner, J., Warwick, N. and Browse, J. 1997, Low-temperature damage and subsequent recovery of *fab1* mutant Arabidopsis exposed to 2 [deg] C, *Plant Physiol*., **113**, 347–56.
63. Gao, J., Wallis, J. G. and Browse, J. 2015, Mutations in the prokaryotic pathway rescue the fatty acid biosynthesis1 mutant in the cold, *Plant Physiol*., **169**, 442–52.
64. Sung, S. and Amasino, R. M. 2004, Vernalization in *Arabidopsis thaliana* is mediated by the PHD finger protein VIN3, *Nature*, **427**, 159–64.
65. Haudry, A., Platts, A. E., Vello, E., et al. 2013, An atlas of over 90,000 conserved noncoding sequences provides insight into crucifer regulatory regions, *Nat. Genet*., **45**, 891–8.
66. Günther, T., Lampei, C., Barilar, I. and Schmid, K. J. 2016, Genomic and phenotypic differentiation of *Arabidopsis thaliana* along altitudinal gradients in the North Italian Alps, *Mol. Ecol*., **25**, 3574–92.
67. De Smet, R., Adams, K. L., Vandepoele, K., Van Montagu, M. C., Maere, S. and Van de Peer, Y. 2013, Convergent gene loss following gene and genome duplications creates single-copy families in flowering plants, *Proc. Natl. Acad. Sci. USA*., **110**, 2898–903.
68. Losada, A., Yokochi, T., Kobayashi, R. and Hirano, T. 2000, Identification and characterization of SA/Scc3p subunits in the *Xenopus* and human cohesin complexes, *J. Cell Biol*., **150**, 405–16.
69. Losada, A., Yokochi, T. and Hirano, T. 2005, Functional contribution of Pds5 to cohesin-mediated cohesion in human cells and *Xenopus* egg extracts, *J. Cell Sci*., **118**, 2133–41.
70. Pezic, D., Weeks, S. L. and Hadjur, S. 2017, More to cohesin than meets the eye: complex diversity for fine-tuning of function, *Curr. Opin. Genet. Dev*., **43**, 93–100.
71. Sumara, I., Vorlaufer, E., Gieffers, C., Peters, B. H. and Peters, J. M. 2000, Characterization of vertebrate cohesin complexes and their regulation in prophase, *J. Cell Biol*., **151**, 749–62.